LHC APERTURE AND ULO RESTRICTIONS: ARE THEY A POSSIBLE LIMITATION IN 2016?

D. Mirarchi*, R. Bruce, M. Giovannozzi, P. Hermes, S. Redaelli,
B. Salvachua, G. Valentino, J. Wenninger , CERN, Geneva, Switzerland

Abstract

Precise knowledge of the available machine aperture is a crucial parameter for the LHC operations. Thus, aperture measurements are performed every year during the machine commissioning, and dedicated Machine Development (MD) runs for validation of possible future optics. A significant beam loss activity in cell 15R8 triggered various studies that revealed the presence of an unexpected aperture restriction due to an Unidentified Lying Object (ULO) in Beam 2. The LHC aperture in 2015 and the unexpected restriction due to the ULO are reviewed in this paper, also in view of their possible impact on 2016 operations.

INTRODUCTION

Historical concerns are present regarding the tight aperture design in the superconducting magnets, with respect to the relatively large beam size at 450 GeV. At 6.5 TeV, the β^* reach is strongly connected with the triplet aperture. Thus, a precise knowledge of the available aperture is crucial to push the machine performance. This is because an adequate protection of bottlenecks has to be ensured at any time by the collimation system, and margins in the collimation hierarchy can be rescaled based on the available machine aperture to ensure both the best cleaning and machine protection performances. An overview on the ULO evolution in 2015, and the proposal on how to minimize his impact for 2016 are discussed. The outcome of aperture measurements at 450 GeV, for proton physics with 80 cm and 40 cm β^* are shown, as well as for ions configuration.

UNIDENTIFIED LYING OBJECT

A significant UFO (Unidentified Falling Object) activity in cell 15R8 was observed during the machine commissioning in 2015. Fast losses at this location led to 14 beam dumps, of which 3 caused a magnet quench. Energy deposition studies showed that the vertex of the hadronic showers is likely situated within 1 m from the center of the dipole MB.C15R8 (B15) [1]. Thus, several local aperture scans were performed around that area (12 in total between April and May) that revealed the presence of the ULO. Different investigations were performed during the year, which were based on three main observables: dedicated local aperture measurements, analysis of UFOs at the ULO location, and parasitic monitoring of beam losses during standard cycles.

* daniele.mirarchi@cern.ch

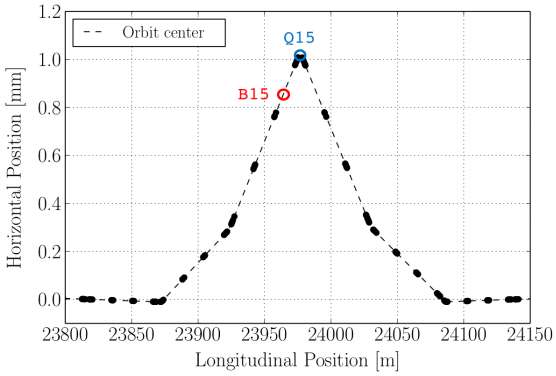

Figure 1: Local orbit bump (3 correctors) for shifts in the horizontal plane. Q15 is enlightened in blue, while B15 in red.

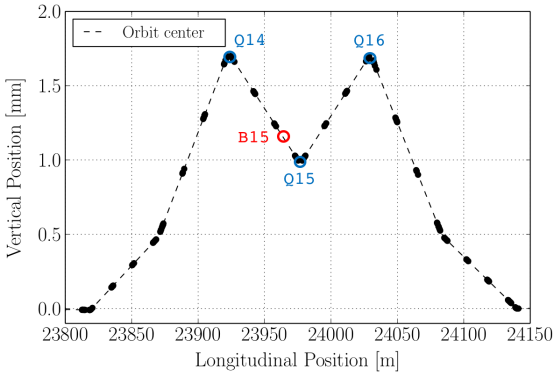

Figure 2: Local orbit bump (4 correctors) for shifts in the vertical plane. Q14, 15 and 16 are enlightened in blue, while B15 in red.

Local aperture measurement procedure

Precise local aperture measurements are performed by means of local orbit bumps. The desired orbit shift is matched at the closest quadrupole (Q15), which is a focusing element. Thus, horizontal shifts are performed using a three-corrector bump (Fig. 1), while in the vertical plane a four-corrector bump is used (Fig. 2). As shown in Fig. 1 and Fig. 2, the actual horizontal orbit shift at the B15 location is 14% smaller than the peak excursions at the adjacent quadrupoles (Q15), while it is 14% larger in the vertical plane. This difference is taken into account in the offline data analysis, in order to reproduce adequately the shape of the ULO.

Aperture measurements are performed by moving the beam towards the aperture until the beam halo "touches" the aperture, as detected by the local beam loss monitors (BLMs). Thus, a precise knowledge of the halo width is necessary. This was achieved by scraping the beam using

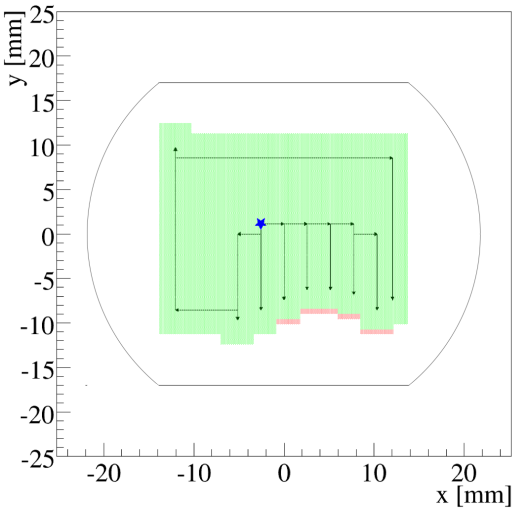

Figure 3: Aperture restriction at the ULO location combining measurements done in April and May 2015. The beam screen it is shown by the black line, black arrows are the path performed by the beam center using local bump, the beam position after the deployment of the fixed bump is shown by the blue star, clear aperture is reported in green while the measured edge of the ULO is shown by red boxes with dimensions equal to the resolution of the measurements.

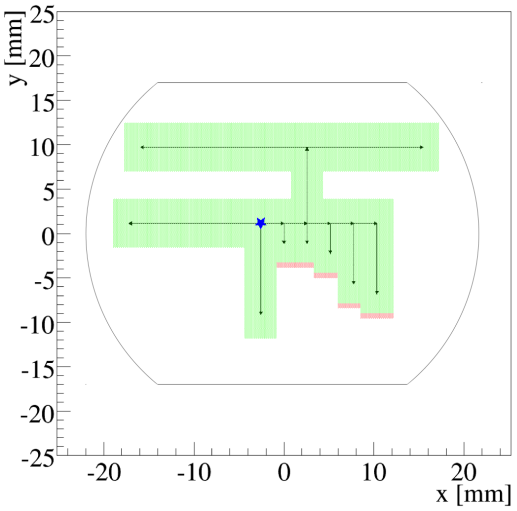

Figure 4: Aperture restriction at the ULO location combining measurements done in November and December 2015, with same color code as in Fig. 3.

primary collimators (TCP) in IR7. In particular, the horizontal and vertical TCP of Beam 2 were closed at 2 σ and 4 σ, respectively. Each time the ULO was touched, the vertical bump was reverted to zero, and a gentle blow up of the beam was performed using the Transverse Damper (ADT) [2]. This ensures that the gap between TCPs was always completely filled, and the beam dimensions were the same in different scans.

With this method, the local aperture was probed systematically by moving the beam to the desired horizontal position, and then scans toward the top and bottom directions were carried out in steps. The step size used was of 0.5 mm and 0.2 mm at 450 GeV and 6.5 TeV, respectively, which correspond to about 0.7 σ, and represent the resolution of the measurement. The maximum bump excursions were:

- ± 14 mm in the horizontal plane, because of losses arising at Q15.
- ± 8 mm in the vertical plane, because of losses arising at Q14 and Q16.

Note that these amplitudes are calculated at the position of the ULO inferred from energy deposition studies [1]. Longitudinal positions of possible obstacles in the bump region cannot be inferred from this measurement.

Main results of local aperture scans

Combining together all the 12 local aperture measurements carried out between April and May 2015, it was possible to reconstruct the transverse shape of the ULO, and a fixed bump of (-3mm, +1mm) in the (H, V) planes was deployed to bypass it. The situation as of May is reported in Fig. 3, were the beam screen is shown in black, black arrows represent the path performed by the orbit center, the beam position after the deployment of the fixed bump is indicated by the blue star, the clear aperture is reported in green while the measured edge of the ULO is delineated by red boxes with dimensions equal to the resolution of the measurements. The available vertical aperture in the worst point (i.e. horizontal bump of 3 mm and 6 mm) it is within 13-14 σ at injection energy, assuming nominal optics.

The Fig. 3 was obtained merging all the scans performed both at 450 GeV and 6.5 TeV that were in agreement within the measurement resolution. However, in few cases also smaller available apertures were measured (i.e. larger vertical dimension of the ULO). These smaller values are still under investigation and are not yet completely understood. Different checks were made both on the offline analysis and during measurements to probe correlations with: intensity, energy, present and previous machine mode. However, no clear correlations were found. Moreover, no clear sign of aperture restriction were observed during standard loss maps and no obvious limitations in operations (losses, collimation cleaning) were present after the deployment of the fixed bumps used to bypass the object.

Other two local aperture measurements were performed toward the end of 2015 (i.e. November and December), with both protons and lead ion beams. Consistent results were obtained in both scans, and the measurements are shown in Fig. 4. As can be easily seen by comparing Fig. 3 and Fig. 4, the vertical dimension of the ULO seem to have increased, while its horizontal width is constant.

Given the rather large vertical dimensions found in these last scans, an evaluation of the available room to increase

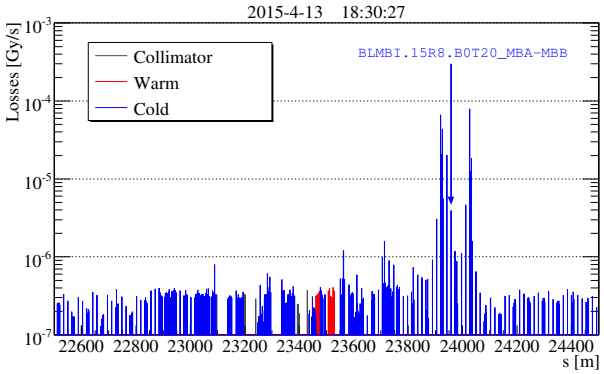

Figure 5: Beam loss in IR8 during the first local aperture scan toward the top of the beam screen. The highest loss spikes occur at the locations of the quadrupoles where the bump is maximum, see Fig. 2.

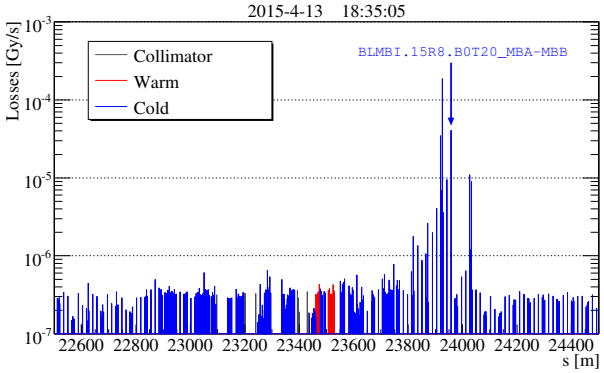

Figure 6: Beam loss in IR8 during the first local aperture scan toward the bottom of the beam screen.

the fixed bump in 2016 was made. These maximum shifts are found to be:

- -6 mm in the horizontal plane.
- +3.5 mm in the vertical plane.

Any combination of horizontal and vertical fixed bump up to the values above ensures at least 10 σ clearance in both planes at 450 GeV, both at the ULO location and at the neighboring MQ used to set up the fixed bump.

Given the high rate of UFO at the ULO location during the first period of operation in 2015, a local thermal cycle of the beam screen was performed. This was intended as an extreme solution to probe the possibility to get rid of this object by evaporation, and its effect is discussed in the next section. On the other hand, one of the main questions was whether this object was present at the bottom of the beam screen from the start of Run II, or if it was initially somehow attached to the top of the the beam screen and fell down after a thermal cycle. This could be evaluated by comparing the two local aperture scans performed before and after the first thermal cycle (done on the 13/4 and the 23/4, respectively). A zoom of beam losses recorded by the BLM in IR8 during the vertical scan toward the top and the bottom, for a zero horizontal shift, are shown in

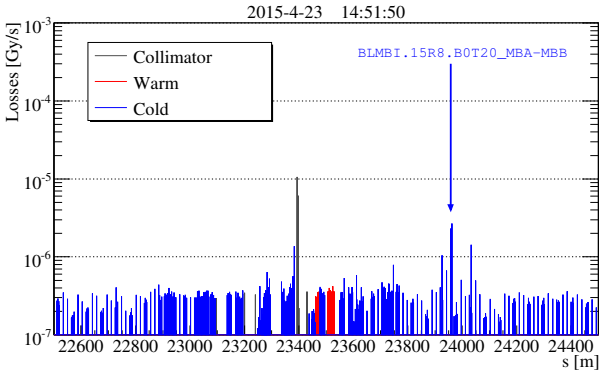

Figure 7: Beam loss in IR8 during the local aperture scan toward the bottom of the beam screen after the first thermal cycle.

Fig. 5 and Fig. 6, respectively. The main BLM that detects hadronic showers due to the interaction of the proton beam with the ULO is the `BLMBI.15R8.B0T20_MBA-MBB` (about 10 m downstream the object in the beam direction [1]), and it is indicated by an arrow. The beam loss pattern obtained by scanning towards the top (Fig. 5) shows a loss pattern consistent with the 4 correctors bump of Fig. 2, with maximum orbit excursions a the adjacent quadrupoles. On the other hand, the scan towards the bottom (Fig. 6) resulted in a significant beam loss at the ULO location while losses appear also at Q14, indicating an obstacle at the ULO location at the very end of the available bump excursion (i.e. bump of -8 mm). Comparing this loss scenario with what was obtained after the first thermal cycle, shown in Fig. 7, for a scan toward the bottom with zero horizontal shift, it is now clear that something is touched much earlier with a bump of about -5 mm (losses on injection protection collimators shall be disregarded because they are due to different settings than in the previous scans). However, it is not possible to conclude that this increase of vertical size was induced by the thermal cycle, because increases of vertical dimension were observed along the year as discussed in the next.

Regarding the possibility that the ULO was there also during Run I, different investigations were performed by looking at local beam loss during orbit shift toward the present position of the object. However, no clear signature were observed mainly because of a significant difference in positions and number of BLMs in that area of the ring.

Other evidence pointing towards the presence of the ULO from the beginning of Run II was also obtained from the parasitic monitoring of beam losses during standard cycles, as discussed in the relative section.

UFO at the ULO

Analysis of the UFO rate at the ULO location was performed by using the UFO Buster application [3]. The ratio of BLM signal at the ULO location with respect to the dump threshold as a function of time is shown in Fig. 8. From this plot one can evaluate the effectiveness of the fixed bump deployed to bypass the ULO, deployed the 29th of April. After

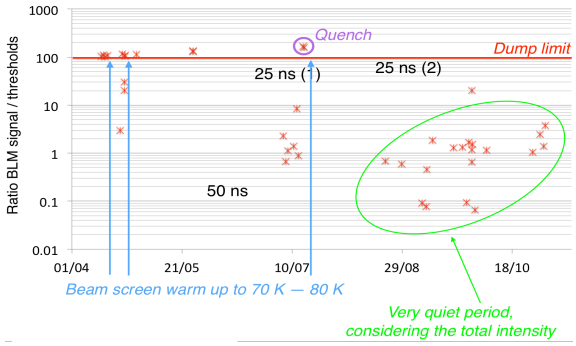

Figure 8: UFO registered by the UFO Buster at the ULO location. The ratio of BLM signal with respect to the dump threshold as a function of the day during the whole proton run in 2015, it is shown.

a significant UFO activity at the beginning the run, the rate of detected UFOs at the ULO location decrease significantly after the set up of the fixed bump. A beam loss induced quench take place on the 14th of July due to a shift of the beam toward the ULO during the energy ramp. However, after this event the UFO activity decreased significantly despite the constantly increased stored intensity in the machine (up to about 280 MJ at the end of 2015 proton run). This behavior is not yet understood.

Parasitic monitoring of beam losses

Beam losses at the ULO location were also continuously monitored during the whole 2015 run. The number of spikes observed by looking at the BLM at the ULO location is shown in Fig. 9, as a function of time. The number of induced dumps it is also reported. Only clear loss spikes using 1.3 s integration time were taken into account, which means spike with a sharp rising front and an exponential decay. In particular only spikes above 1×10^{-6} [Gy/s] were considered, because of a background level at this BLM of about 5×10^{-7} [Gy/s]. Most of these spikes were synchronized with beam injection or injection cleaning, whereas the ones that took place at 6.5 TeV (or during the energy ramp) caused a beam dump. The times of thermal cycles of the beam screen are indicated by green lines, the moment when the fixed bump was deployed is indicated by a red line, and the scrubbing runs are in blue. The main outcome of this analysis is:

- In the first day of circulating beam in the LHC (i.e. 5th of April) as many spikes as the number of injections performed were recorded, synchronized with the beam injections. This is another confirmation that the ULO was there from the beginning of Run II.

- Conclusions cannot be drawn on the effect of the beam screen thermal cycle, because no clear difference in spike rate is observed before and after they were performed. This observation is not fully consistent with the fact that UFO rates improved immediately after the first thermal cycle.

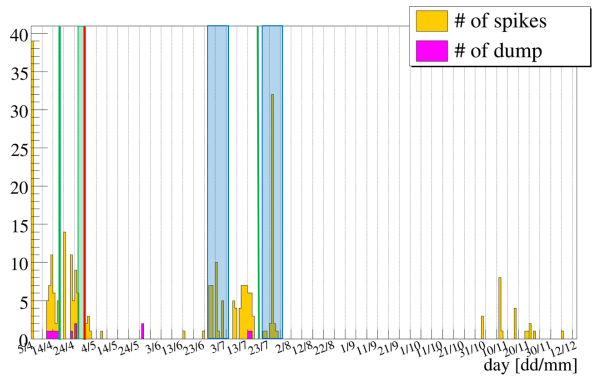

Figure 9: The number of spikes observed at the ULO location and induced beam dump as a function of the day, during the whole 2015 run. Days in which a thermal cycle of the beam screen was performed are shown by green lines, while the day in which the fixed bump was deployed is indicated by a red line, and the scrubbing runs are in blue.

- After an initial violent activity during the beam commissioning, a significant decrease of loss rate is observed thanks to the setup of the fixed bump (i.e. 29th of April).

- A relatively quiet period follows the deployment of the bump. However, two beam dumps (i.e. 25th of May) took place after a relatively hard scraping on the object, indicating that the possibility to burn it with intense beam could be dangerous.

- A violent reactivation of beam loss at the ULO location it is observed during the scrubbing runs for 50 ns and 25 ns physics.

- No activity is observed after the scrubbing runs until the end of October, when beam manipulations during dedicated MD and standard operations led to a beam growth and/or orbit shift toward the ULO.

AVAILABLE LHC APERTURE

Aperture measurements are performed every year during the machine commissioning, and dedicated MD runs to validate present and future optics. They rely on different measurement procedures, depending on the machine mode in which the available aperture is probed, which are described in the relative subsection that follow.

Aperture at Injection

Two methods are used for this machine mode: first a global aperture measurement is performed in order to identify bottleneck in the machine, and then local aperture measurements are performed at these locations.

Regarding the global aperture measurements, the main steps followed are:

1. TCPs in IR7 are closed to the desired aperture (i.e. 8 σ).

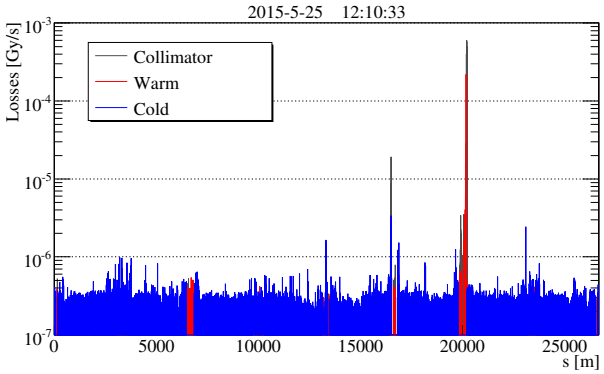

Figure 10: Example beam loss around the whole ring during global aperture measurements, with primary collimators in IR7 still bottleneck of the machine.

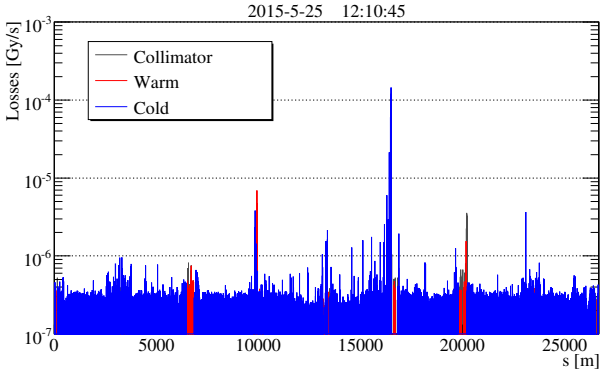

Figure 11: Example beam loss around the whole ring during global aperture measurements, with primary collimators in IR7 retracted just enough to identify the aperture bottleneck of the machine.

2. Gentle transverse blow up is performed using the ADT.

3. TCPs in IR7 are opened of 0.5 σ with following beam blow up.

4. Steps 2 and 3 are repeated until the loss location moves from the TCP to the machine bottleneck.

This procedure is carried out separately for horizontal and vertical planes of the two beams. An example of losses around the whole ring before and after the identification of the bottleneck are shown in Fig. 10 and Fig. 11, respectively. Together with the identification of the longitudinal position of the bottleneck, this procedure also provides a first evaluation of the available aperture at that point of the machine. This is given by the TCP aperture at the first step in which beam loss move to the bottleneck. However, local measurements are performed to have a more precise evaluation of this aperture. The main steps followed are:

1. TCP in IR7 are closed to shape the beam at the desired aperture (i.e. 4 σ).

2. A local orbit bump is matched with maximum at the global bottleneck found earlier.

Table 1: Machine bottleneck at 450 GeV and relative aperture, in 2012 and 2015.

	2015		**2012**	
	A [σ]	**Element**	**A [σ]**	**Element**
B1H	11.6	MBRC.4R8	11.5	Q6R2
B1V	12.4	Q6L4	12.0	Q4L6
B2H	13.0	Q4L6	12.5	Q5R6
B2V	12.7	Q4R6	12.5	Q4R6

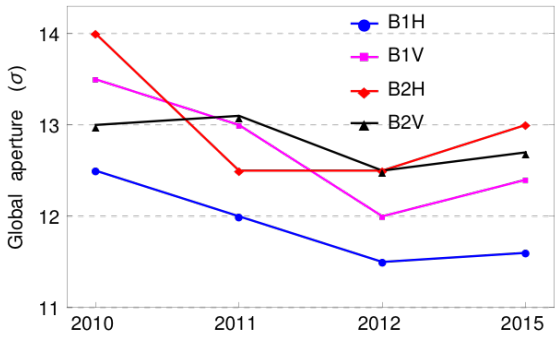

Figure 12: Evolution of minimum available aperture at 450 GeV during the years.

3. The local bump is increased in steps of 0.5 σ until beam losses are observed.

4. Step 3 it is repeated for both sign of the bump (i.e. in case of horizontal bottleneck toward the inner and outer side of the machine, while for the vertical ones toward the top and the bottom).

Moreover, this technique allow us to re-centre the beam in case an asymmetry is found. Thus, allowing to gain aperture by means of a local fixed bump in order to maximize the available aperture at the bottleneck found.

A summary table of restrictions found and relative aperture is given in Table 1. A comparison with respect to what found during the last measurements of Run I in 2012 is also reported. In both cases the smallest values found with the two methods described above are reported, with resolution of 0.5 σ. The evolution of the minimum aperture from 2010 to 2015 it is shown in Fig. 12. As can be seen from Fig. 12 some aperture was gained with respect to 2012, but not as much as in 2010. The decrease of aperture from 2010 to 2012 can be due to small variation in the magnets positions during Run I, while the increment observed in 2015 can be due to the adjustments performed during LS1.

Aperture in Physics

With squeezed beams at top energy, the machine bottleneck moves automatically to the magnets of the triplets (MQX), where the largest values of the beta function are present. The technique used is very similar to that for global aperture measurements at injection energy, but using tertiary collimators (TCTs) instead of TCPs and all the collimation

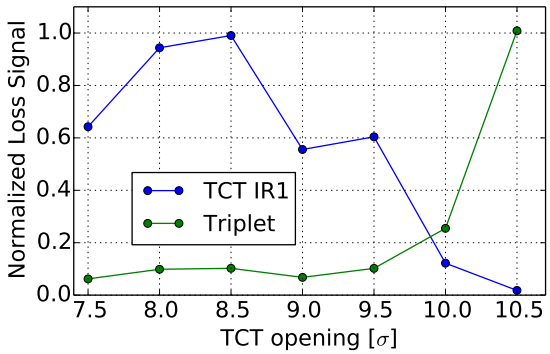

Figure 13: Example of offline analysis from where the available triplet aperture can be evaluated (B2V, 40 cm β^*). Losses at the TCT and at the relative triplet are first normalized to the intensity lost for each beam excitation, then normalized to the highest value, and plot as a function of the TCT aperture.

system in garage position. Similarly to global aperture measurements at injection, TCTs in IR1 and IR5 are opened in steps of 0.5 σ until beam loss move from the TCTs to MQXs, indicating that the triplet is exposed. An example of offline analysis is given in Fig. 13, where the raw data are first normalized to the intensity lost for each beam excitation (because BLM signal are proportional to it), and then normalized to the highest value (because of different BLM response as a function of the local geometry). Thus, the available aperture at the triplet is given by the intersection point of the two lines.

These measurements were performed during the protons and ion beam commissioning with 80 cm β^*, and during dedicated MD runs for protons physics with 40 cm β^* foreseen for 2016. Summary tables are given in Tab. 2 and Tab. 3 for protons and ions physics, respectively.

It is important to note that a good agreement with predictions based on Run I experience was found, where the smallest apertures expected were 15.9 σ with 80cm β^* and 9.5 σ with 40cm β^* [4]. The aperture for the ion configuration with also IR2 squeezed to 80 cm was measured by stopping the scans at 15.5 σ. However, a smaller aperture than expected was found in the vertical plane. This could be partially explained with an orbit drift that was not corrected, in combination with beta beating. However, these measurements will be performed again during the 2016 machine commissioning to confirm the available aperture of the triplet, to then decide which optics will be used in 2016 (i.e. 40 cm β^*, 80 cm β^*, or intermediate step) .

CONCLUSIONS

The presence of the ULO since the beginning of 2015 has been confirmed. However, it is not possible to conclude on its presence also during Run I (no interventions were made in that area during LS1) because of the significantly different BLM layout. Although initial concerns (14 dump, 3 quench during machine commissioning) beam loss at the ULO were

Table 2: Machine bottleneck for protons physics and relative aperture, with 80 cm and 40 cm β^*.

	80 cm β^* 145 μrad Xing		**40 cm β^* 205 μrad Xing**	
	A [σ]	**IR**	**A [σ]**	**IR**
B1H	16.7	5	11.0	5
B1V	15.7	1	9.5	1
B2H	> 18.7	-	10.0	1
B2V	15.7	1	9.5	1

Table 3: Machine bottleneck for ions physics and relative aperture, with 80 cm β^*.

	80 cm β^* 145 μrad Xing	
	A [σ]	**IR**
B1H	> 15.5	-
B1V	14.0	1
B2H	> 15.5	-
B2V	14.0	2

not a limitation in 2015, thanks to the effectiveness of the fixed bump deployed to bypass it. However it is hard to predict the situation in 2016 because of lack in understanding the nature of the object. Nevertheless, in the worst scenario where it keeps increasing its vertical dimensions, there is still room to increase the fixed orbit bump to obtain a least 10 σ at 450 GeV in both planes. Thus, it will be crucial to perform detailed local aperture scans during the 2016 commissioning, in order to setup the optimum orbit bump. Moreover continuous beam loss monitoring and periodic ULO scans could be very useful to avoid any limitation to LHC operations.

Regarding the available machine aperture, the worst cases found are: at injection an aperture of 11.6 σ in the horizontal plane of a recombination dipole in IR8; for proton physics configurations the smallest aperture found are 15.7 σ with 80 cm β^*, 9.5 σ with 40 cm β^*, for both beams in the vertical plane of IR1, well in agreement with predictions based on Run I experience; with ions beams and in physics configuration the available aperture was found to be 14 σ, in the vertical plane of IR1 and IR2 for beam 1 and beam 2, respectively. Global and local aperture measurements, both at injection and top energy, are required during 2016 commissioning to check bottleneck evolution and to avoid any limitation to LHC operations.

ACKNOWLEDGMENT

The authors would like to thank the BE-OP group for the support during measurements, and the BE-ABP group for the useful internal discussions. In particular thanks to A. Mereghetti, P. Skowronski, A. Valloni, H. Garcia and R. Kwee-Hinzmann for their participation to the aperture measurements.

REFERENCES

[1] A. Lechner et al., “Beam induced quenches update", LMC 22nd April 2015

[2] W. Hofle et al., “Controlled Transverse Blow-UP of high-energy proton beams for aperture measurements and loss maps", Proceedings of IPAC12, N. Orleans, USA

[3] T. Baer et al., “UFOs in the LHC", Proceedings of IPAC11, San Sebastian, Spain

[4] R. Bruce et al., “Baseline Machine Parameters and Configuration for 2015", Chamonix workshop 2014